Available online at www.sciencedirect.com
SCIENCE DIRECT®
Nuclear Instruments and Methods in Physics Research A 551 (2005) 448–457
NUCLEAR INSTRUMENTS & METHODS IN PHYSICS RESEARCH Section A
www.elsevier.com/locate/nima

Development of a wide-range paired scintillator with optical fiber neutron monitor for BNCT irradiation field study

Masayori Ishikawa[a,*], Hiroaki Kumada[b], Kazuyoshi Yamamoto[b], Junichi Kaneko[c], Gerard Bengua[d], Hironobu Unesaki[d], Yoshinori Sakurai[d], Kenichi Tanaka[e], Toshiso Kosako[f]

[a]*Department of Nuclear Engineering and Management, Graduate school of Engineering, The University of Tokyo, Japan*
[b]*Japan Atomic Energy Research Institute, Japan*
[c]*Graduate school of Engineering, Hokkaido University, Japan*
[d]*Research Reactor Institute, Kyoto University, Japan*
[e]*Research Institute for Radiation Biology and Medicine, Hiroshima University, Japan*
[f]*Department of Nuclear Professional School, Graduate school of Engineering, The University of Tokyo, Japan*

Received 24 May 2005; received in revised form 14 June 2005; accepted 15 June 2005
Available online 6 July 2005

Abstract

A wide range thermal neutron detector was developed based on the Scintillator with Optical Fiber (SOF) detector which has been previously used for thermal neutron monitoring during boron neutron capture therapy irradiation. With this new detector system we intended to address the issues of real-time thermal neutron flux measurement and the simultaneous measurement of a wide range of thermal neutron flux in a BNCT irradiation field which were difficult to implement with the gold wire activation method.

The dynamic range of linearity of the SOF detector was expanded by using a plastic scintillator with a rapid decay time. On the other hand, the contribution of gamma rays and fast neutrons in the measured signals were compensated from those obtained by a pair of SOF detectors, one with a ^{6}LiF neutron converter and the other without. The discrimination level for the measured signals was also optimized to further reduce the contribution of gamma rays and fast neutrons signals. A non-paralyzable system model was applied to correct for the dead-time in the detector system.

A good agreement between the thermal neutron flux measured by the gold wire activation method and the paired SOF detector system was observed. However, measurements which would normally take a few days to perform with the

*Corresponding author. Tel.: +81 3 5841 2988; fax: +81 3 5841 2928, +81 3 3815 8540.
E-mail address: masayori@n.t.u-tokyo.ac.jp (M. Ishikawa).

0168-9002/$ - see front matter
doi:10.1016/j.nima.2005.06.044

gold wire activation method were obtained in just about 15 min using the SOF detector system. We also confirmed the dynamic range of linearity for the SOF detector system to be in the order of magnitude of 10^4.

PACS: 87.66.−a; 87.53 Pb; 87.53.Qc

Keywords: SOF detector; Ultra-miniature detector; Thermal neutron monitor; Phantom experiments; BNCT

1. Introduction

There are many detectors used for thermal neutron monitoring such as the $^{10}BF_3$ or ^3He gas counter, fission chambers and the ^6Li-doped photodiode detector [1]. Recently, a new type of detector using a scintillator coupled to an optical fiber was developed for the same purpose [2]. Among these types of detectors, the Scintillator with Optical Fiber (SOF) detector has been used for monitoring thermal neutrons during boron neutron capture therapy (BNCT) irradiations in Japan [3]. The detector probe of the SOF detector system is smaller than the other neutron monitors which makes it more useful for thermal neutron monitoring in narrow spaces.

The SOF type detector was originally developed by Mori [1]. Mori's detector used a mixed powder of ^6LiF and ZnS(Ag) as scintillator. In this detector system the scintillation signals were converted to electric pulses via a photo-multiplier tube and then the discriminated pulses were counted to eliminate gamma-ray signals. Mori's detector system worked well except for one limitation which was the dependence of the measured gamma-ray contribution on the amount of incident gamma rays.

In the neutron irradiation field for BNCT, thermal neutron flux could vary from 10^6 to almost 10^{10} n/cm^2/s. The gold wire activation method has been routinely used to measured thermal neutron flux distribution in a BNCT irradiation field but real-time measurements using this method are difficult to implement. Moreover, simultaneous measurement of such a wide range of thermal neutron flux with activation method is not easy to carry out.

In this paper, we will report an upgrade of the SOF type detector by using a plastic scintillator. A plastic scintillator has a relatively rapid decay time (in the order of a few nanoseconds) which is expected to expand the detector's dynamic range of linearity.

2. Detector characteristics

2.1. Detector composition

Shown in Fig 1 is a schematic illustration of the SOF detector system. The SOF detector consists of a small amount of plastic scintillator, a plastic optical fiber, a photo-multiplier tube, a charge pre-amplifier, a discriminator and a counter. In this research, we used a BC490 plastic scintillator manufactured by Bicron Ltd. The BC490 is partially polymerized and hardened with a catalyst and this makes it possible to be tightly connected to the tip a plastic optical fiber (Mitsubishi Rayon MH4001, 1 mm-diameter optical fiber with 2.2 mm-diameter polyethylene shielding). A small amount of LiF powder (enriched 95% ^6Li) is then painted over the plastic scintillator. The reactions between ^6Li nuclei and thermal neutrons emit charged particles (alpha and triton) which produce scintillation photons in the plastic scintillator. The photon signals are relayed through the optical fiber onto the Photon Counting Unit (Hamamatsu H7155) and then converted into 30 ns-width TTL pulses. The counting unit is made up of a photo-multiplier tube, charge pre-amplifier and discriminator. The pulse counts are sent to a personal computer via a universal serial bus (USB) connection. By setting an adequate discrimination level, a small or negligible gamma-ray contribution could be achieved since a plastic scintillator has a small cross-section for photo-electric reactions.

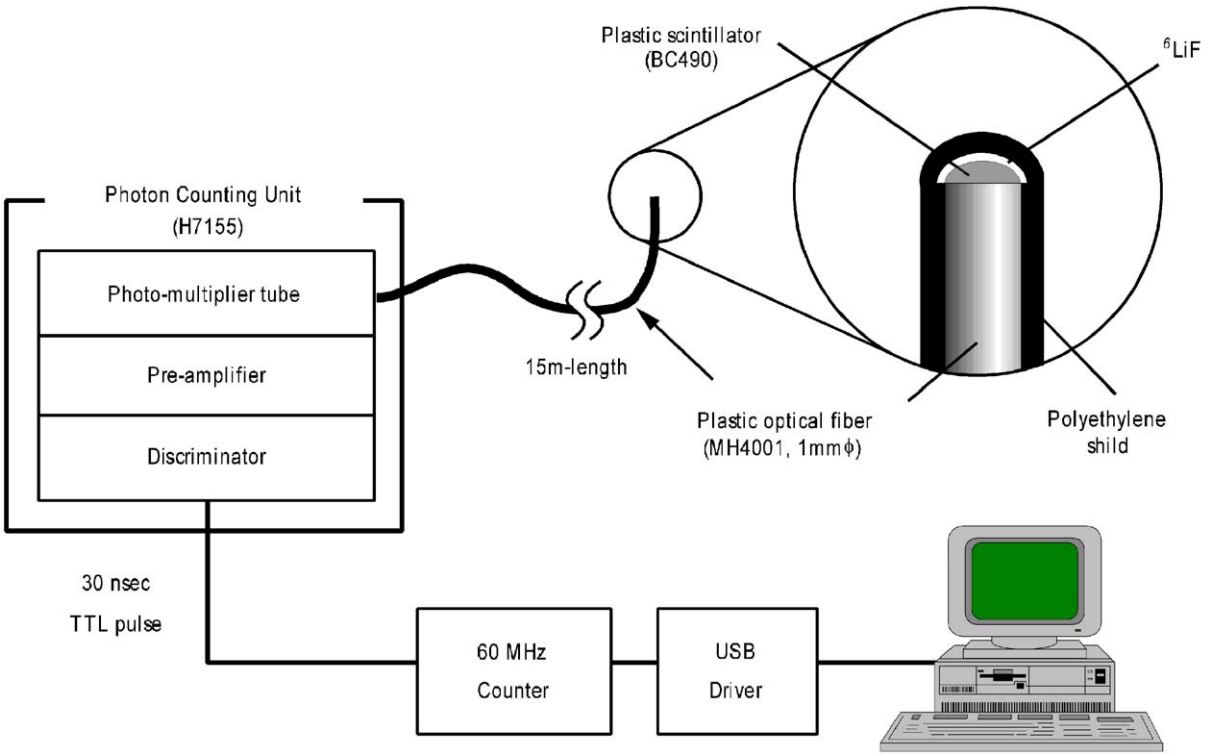

Fig. 1. Schematic diagram of SOF detector system. The SOF detector made up of a small plastic scintillator with ^{6}LiF, a plastic optical fiber, a photon counting unit and data acquisition system connected to personal computer via USB.

2.2. Performance test

To evaluate our SOF detector, a linearity test was performed using the JRR-4 Medical irradiation facility at the Japan Atomic Energy Research Institute (JAERI). Fig. 2 shows the experimental setup for the linearity performance test. The detector probe was placed in an 18.6 cm $\phi \times 24$ cm water-filled phantom whose walls were made from a 3 mm thick polymethylmetacrylate (PMMA) to enhance thermal neutron flux. The dynamic range of linearity for the SOF detector was investigated by varying the reactor power. The thermal neutron flux at the point of measurement ranges from 2×10^4 to 3×10^9 n/cm^2/s depending on the reactor power which can be set at 20 W to 3.5 MW. Gamma-ray flux was also found to be dependent on the reactor power; however, the variation in the gamma flux with respect to the reactor power was not linear because of the strong gamma rays coming from the reactor core.

Fig. 3 shows the measured count rate as a function of the reactor power at TNB-1 irradiation mode (see Table 1). With the reference point set at 20 kW, non-linearity was observed under 2 kW and over 200 kW. The non-linearity below 2 kW could be attributed to gamma rays and/or fast neutrons because the measured count rate by the SOF detector was larger relatively to the expected count rate at this range of the reactor power. On the other hand, the non-linearity over 200 kW could be due to count-drop which may occur at a high counting rate because the measured count rate by the SOF detector was smaller relative to what is expected at this range of the reactor power. As a result, the dynamic range of linearity was limited in the order of magnitude of 10^2.

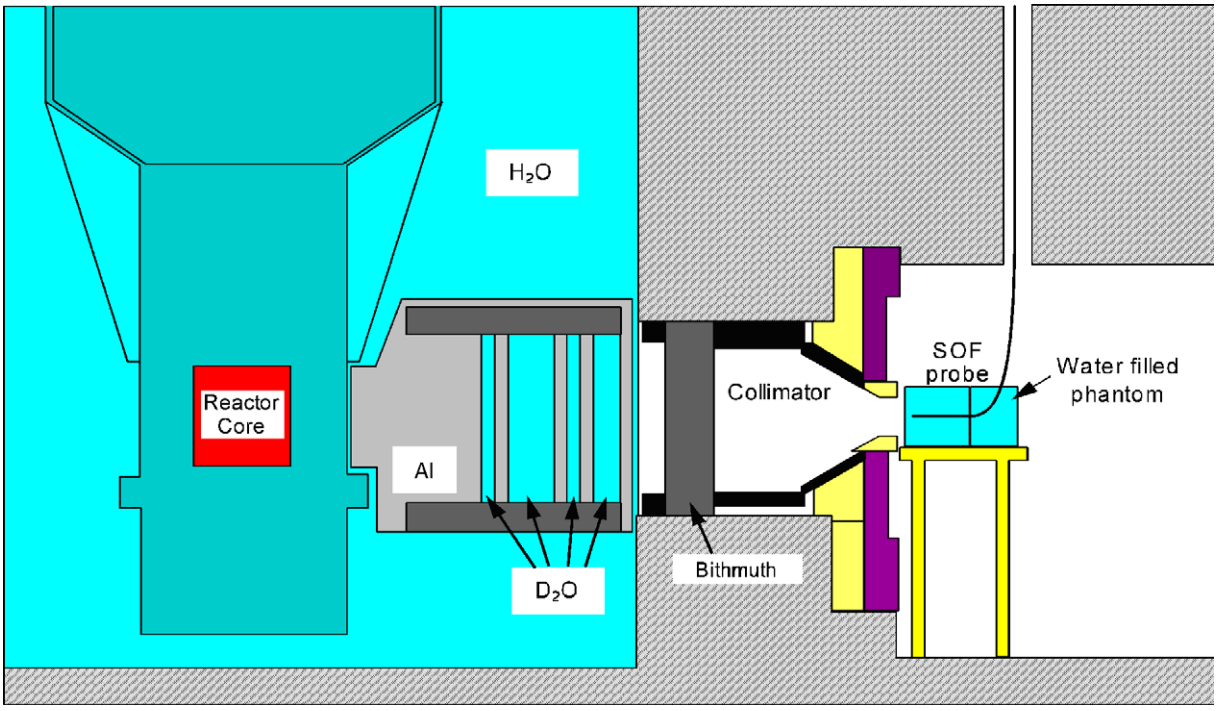

Fig. 2. Experimental setup at JRR-4 medical irradiation facility The detector probe was placed in an 18.6 cm ∅ × 24 cm water-filled phantom whose walls was made from a 3 mm thick polymethylmetacrylate (PMMA) to enhance thermal neutron flux.

3. Upgrading SOF detector

3.1. Compensation of gamma-ray and fast-neutron contributions

A compensation method for the SOF detector for gamma rays was previously reported by Ishikawa [3]. Fig. 4 shows the pulse height spectrum in a neutron irradiation field taken by a BC490 plastic scintillator with and without a ^{6}LiF neutron converter. The solid line is the spectrum measured by the BC490 with ^{6}LiF, which includes thermal neutron, gamma-ray and fast neutron signals. It is sometimes difficult to completely eliminate the gamma-ray or fast neutron contribution in the spectrum even if the discrimination level is set high enough.

The dashed line in Fig. 4 gives the measured spectrum by the BC490 without ^{6}LiF which includes gamma-ray and fast-neutron signals.

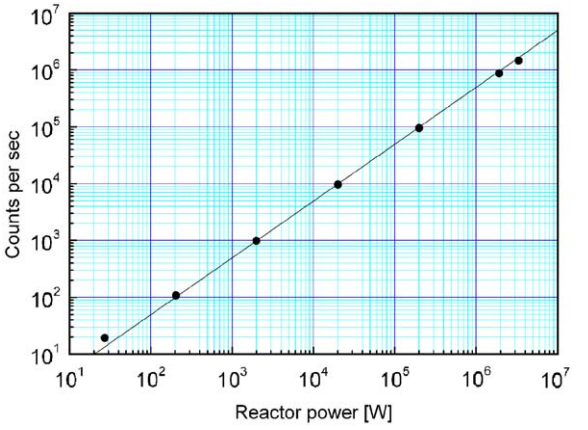

Fig. 3. The measured count rate as a function of the reactor power. Non-linearity was observed under 2 kW and over 200 kW.

The gamma-ray and fast neutron contribution can be delineated and compensated from the difference between the signals obtained from the

Table 1
Characteristics of JRR-4 medical irradiation facility (collimator size: 15 cm, free beam)

Irradiation mode	D_2O thickness (cm)	Cadmium filter	Neutron flux (n/cm^2/s)			Cadmium ratio	Gamma ray (Gy/h)
			Thermal ~0.53 eV	Epithermal 0.53–10 keV	Fast 10 keV~		
ENB	8	On	3.6×10^8	2.2×10^9	9.5×10^7	1.15	0.19
TNB-1	12	Off	2.0×10^9	9.0×10^8	2.7×10^7	2.5	0.24
TNB-2	33	Off	6.5×10^8	3.2×10^7	6.2×10^5	13.5	0.47

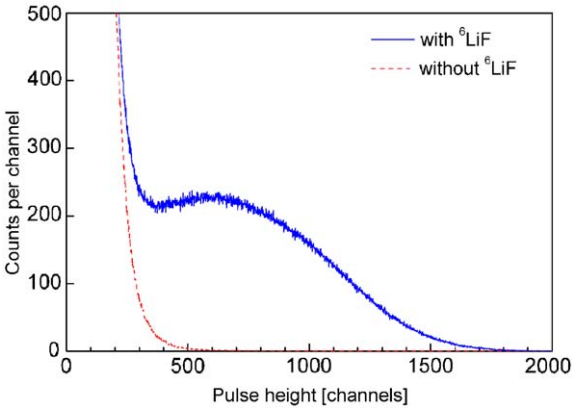

Fig. 4. The pulse height spectrum of a BC490 plastic scintillator with and without ^{6}LiF neutron converter in a neutron irradiation field. The solid line is the spectrum measured by the BC490 with ^{6}LiF, and the dashed line is that of without ^{6}LiF.

scintillator without ^{6}LiF and the signals from the scintillator with ^{6}LiF.

3.2. Theory of compensation

Fig. 5 shows a schematic diagram of the paired SOF detector system. The signal processing of the paired SOF detector is exactly the same as that of a single SOF detector. As shown in Fig. 5, the paired SOF detector is composed of two BC490 scintillators, one with ^{6}LiF and the other without ^{6}LiF. Both scintillators, with and without ^{6}LiF, were connected to a paired plastic optical fiber (MH4002, Mitsubishi Rayon) and coated with a reflector paint (BC620, Bicron Ltd.). The sizes of the scintillators were not perfectly identical owing to the difficulty in their construction. This difference led to a different efficiency for each detector. Other possible differences between the paired SOF detectors could be due to the transmission loss of optical fiber, gain of photomultiplier tubes and slightly different discrimination level. In order to account for the difference in the relative efficiencies of the detectors, correction factors for the measured counts by each detector were introduced. The measured counts for the scintillator with and without ^{6}LiF were assumed to be expressible in terms of Eqs. (1) and (2), respectively:

$$C_+ = R_{n+}F_n + R_{g+}F_g + R_{f+}F_f \quad (1)$$

$$C_- = R_{g-}F_g + R_{f-}F_f. \quad (2)$$

In Eq. (1), C_+ represents the measured counts of the scintillator with ^{6}LiF. This is given here as the sum of the corresponding products between the particle fluence (i.e, F_n, F_g, and F_f) and the detector response factor (i.e., R_n, R_g, and R_f) for thermal neutrons, gamma rays and fast neutrons. In Eq. (2), C_-, R_{g-}, and R_{f-} are the measured counts, response factor for gamma rays and fast neutrons, respectively, for the scintillator without ^{6}LiF.

The response factors R_{g+} and R_{g-} were obtained from the measured counts of both detectors when only a gamma ray field was used following Eqs. (3) and (4). Here, C'_+ and C'_- are the measured gamma ray counts for the detectors with and without the neutron converter, respectively. These correction factors were determined from measurements using an intense pure

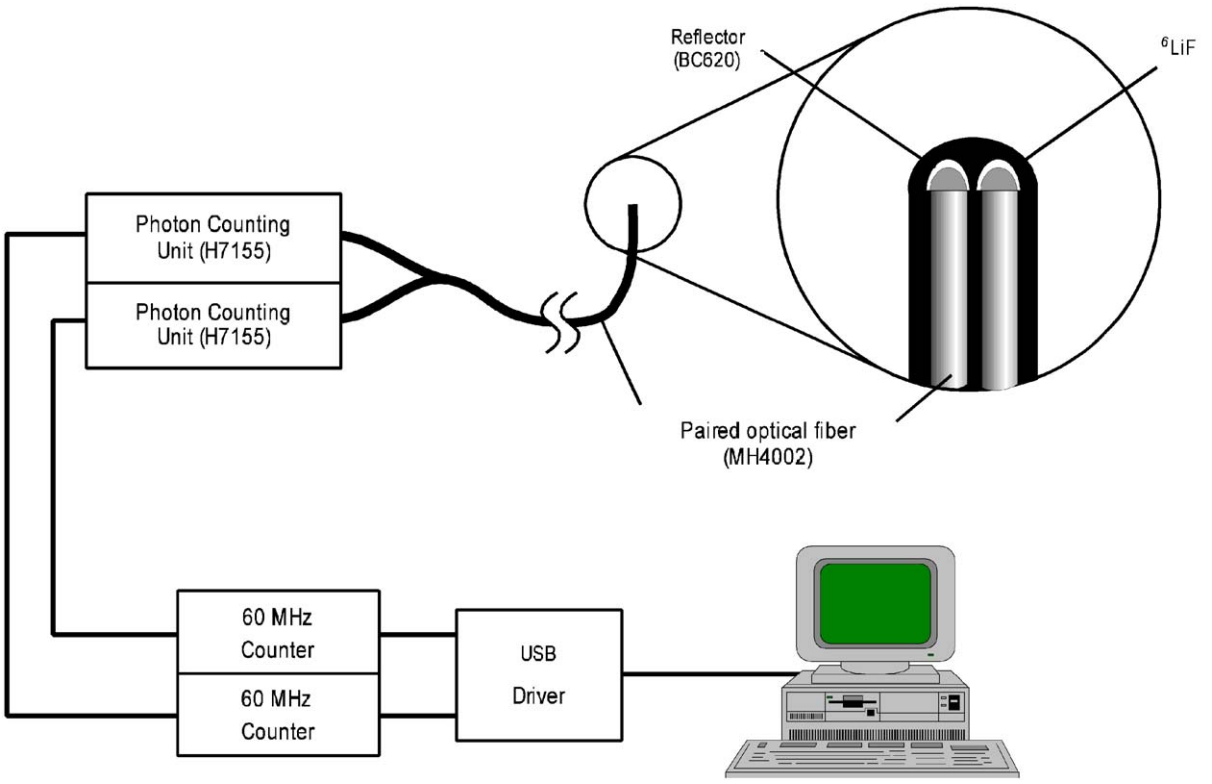

Fig. 5. Schematic diagram of the paired SOF detector system. The signal processing of the paired SOF detector is exactly same as that of a single SOF detector. The paired probe consists of BC490 plastic scintillator with and without ^{6}LiF.

gamma-ray source such as ^{137}Cs:

$$C'_+ = R_{g+}F'_g \tag{3}$$

$$C'_- = R_{g-}F'_g. \tag{4}$$

The response ratio R_{g+}/R_{g-} can be expressed in terms of C'_+ and C'_- from Eqs. (3) and (4).

The response factors R_{f+} and R_{f-} should be proportional to R_{g+} and R_{g-}, respectively, since the detector responses were only influenced by the scintillator volume. Accordingly, the response ratio R_{f+}/R_{f-} should be equal to R_{g+}/R_{g-}. From these four equations, we obtain C_+ in the form

$$C_+ = R_{n+}F_n + \frac{R_{g+}}{R_{g-}}C_- = R_{n+}F_n + \frac{C'_+}{C'_-}C_-. \tag{5}$$

The expression for the neutron flux F_n can then be deduced from Eq. (5) and is given by

$$F_n = \frac{C_+ - (C'_+/C'_-)C_-}{R_{n+}}. \tag{6}$$

3.3. Optimization of discrimination level

If the discrimination level is high enough, the contribution of gamma rays and fast neutrons will be small. However, the amount of thermal neutron signals will also be small because many thermal neutron signals are discarded. Therefore, we tried optimizing the discrimination level by considering counting statistics. We rewrite Eq. (6) in the form

$$F_n = \frac{C_+ - (R_{g+}/R_{g-})C_-}{R_{n+}} = \frac{1}{R_{n+}}C_+ - \frac{R_{g+}}{R_{n+}R_{g-}}C_-. \tag{7}$$

The standard deviation of the evaluated thermal neutron flux σ_{F_n} is given as follows.

$$\sigma_{F_n} = \sqrt{\left(\frac{1}{R_{n+}}\right)^2 \sigma_{C_+}^2 + \left(\frac{R_{g+}}{R_{n+}R_{g-}}\right)^2 \sigma_{C_-}^2} = \frac{\sqrt{C_+}}{R_{n+}} \sqrt{1 + \left(\frac{R_{g+}}{R_{g-}}\right)^2 \frac{C_-}{C_+}}. \quad (8)$$

Here, σ_{C_+} and σ_{C_-} are the standard deviations of the measured count of the scintillators with and without the neutron converter, respectively. The relative standard deviation is given by

$$\sigma_{F_n}/F_n = \frac{1}{\sqrt{C_+}} \sqrt{1 + \left(\frac{R_{g+}}{R_{g-}}\right)^2 \frac{C_-}{C_+}} \Bigg/ \left(1 - \frac{R_{g+}}{R_{g-}} \frac{C_-}{C_+}\right). \quad (9)$$

Fig. 6 shows the relative standard deviation as a function of the discrimination level under the same condition as in Fig. 4. From Fig. 6, it was found that the relative standard deviation is minimized at around 300 channels. However, the discrimination level was set to 500 channels for the succeeding experiments because the minimum point appeared to shift slightly higher as the gamma-ray contribution increases.

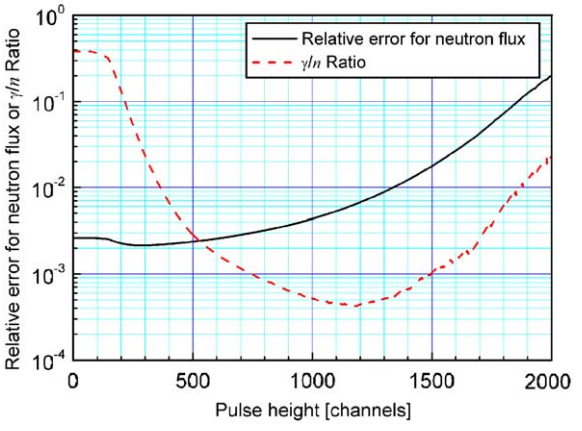

Fig. 6. The relative standard deviation as a function of the discrimination level. The relative standard deviation is minimized at around 300 channels.

3.4. Confirmation of compensation

As pointed out in the previous section, the SOF detector system requires the conversion coefficient R_{n+} and the R_{g+}/R_{g-} ratio to evaluate thermal neutron flux. An R_{g+}/R_{g-} ratio of 0.9556 was obtained from a ^{137}Cs gamma-ray source (62 TBq) while a conversion coefficient R_{n+} of 2.072×10^3 was obtained from the thermal neutron irradiation field at JRR-4.

A linearity test for the paired SOF detector was performed at JRR-4 with the same conditions for a single SOF detector experiment. Fig. 7 shows the result of the linearity performance test with the paired SOF detector. From Fig. 7, the compensation effect was observed below 2 kW, and the linearity for the paired SOF detector was guaranteed from 200 W to 200 kW.

3.5. Dead-time correction

Generally, dead-time correction for the pulse counting method is applied when a high counting rate is used. This correction can be carried out using a paralyzable system model or non-paralyzable system model. For our detector system dead-time can occur while discriminating the output of the photo-multiplier and during the counting of

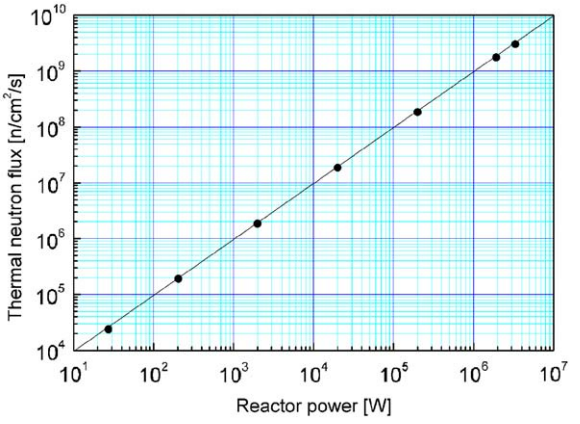

Fig. 7. The result of linearity performance test with paired SOF detector. The compensation effect was observed under 2 kW, and the linearity for the paired SOF detector was guaranteed from 200 W to 200 kW.

the TTL pulses from the photon counting unit. These processes appear to obey a non-paralyzable behavior; thus, a non-paralyzable system model was adapted for the dead-time correction in the SOF detector system.

The true count rate for the non-paralyzable system model is expressed by

$$n = \frac{m}{1 - m\tau}. \tag{10}$$

Here m stands for the observed count rate and τ for the dead time. To estimate the dead time of the SOF detector system, a Light Emitting Diode (LED) with peak wavelength similar to a plastic scintillator (420 nm) was used as a signal source in place of the scintillation signal. The LED was driven by a 300 MHz arbitrary waveform generator (Wavetek Model 302) which generated light pulses similar to a real scintillation pulse. The dead time of the SOF system was evaluated by changing the generated pulse rate. Fig. 8 shows the pulse counting rate as a function of generated pulse rate. The solid circles show the raw counting rate of the SOF detector. By fitting this data into Eq. (10), the dead time of this system was evaluated to be $\tau = 23.62$ ns. The dashed line in Fig. 8 represents the pulse rates with missed counts as a result of a dead-time $\tau = 23.62$ ns. The open circles in Fig. 8

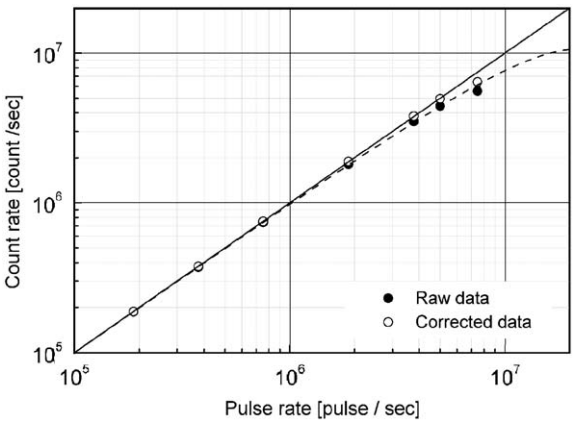

Fig. 8. The pulse counting rate as a function of generated pulse rate. Solid circle and open circle indicate the raw counting rate of SOF detector and the corrected value with non-paralyzable system model, respectively. The dashed line represents the function of the pulse rate with non-paralyzable system model.

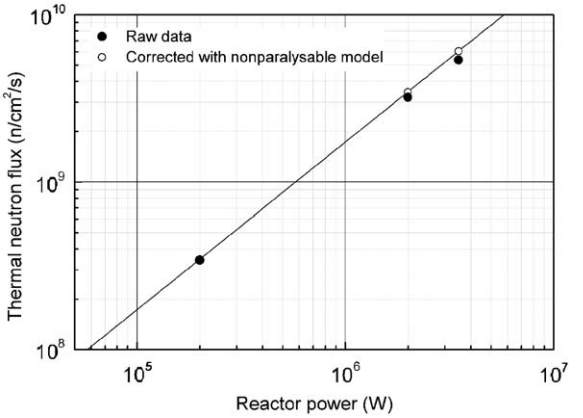

Fig. 9. The linearity experiment data corrected with non-paralyzable system model. A good linearity was observed up to 3.5 MW.

are the corrected pulse rates computed based on Eq. (10). These data are in good agreement with the real pulse rate of 5×10^6 pulse per second (pps). For the probe used in this research which has a conversion coefficient of 2.072×10^3, the dead-time correction can be used for neutron fluxes of up to 10^{10} n/cm^2/s.

Fig. 9 shows the data for the linearity experiment corrected with the non-paralyzable system model. The data sets were completely the same as in Fig. 7. A good linearity was observed up to 3.5 MW in Fig. 9. Accordingly, the SOF system has a linearity range from 2×10^5 to 3×10^9 n/cm^2/s which indicates that the dynamic range of linearity was guaranteed in the order of magnitude of 10^4.

4. Application for evaluation of neutron field

In order to verify the feasibility of using the SOF detector with modifications mentioned earlier, thermal neutron measurements were performed at the JRR-4 irradiation facility. Our benchmark for the evaluated characteristics of JRR-4 irradiation facility were those reported by Yamamoto [4] for the thermal neutron distribution along with center axis of water-filled phantom using the gold wire activation method. For consistency of set-up, we used

the same water-filled phantom used by Yamamoto in this research. Since gamma-ray flux distribution is not proportional to thermal neutron flux distribution, it was possible to perform measurements that would confirm the effectiveness of the correction method for gamma ray. Additionally, we were able to check the dynamic range of linearity of the SOF by varying the thermal neutron flux range from 10^6 to 5×10^9 n/cm^2/s by using alternating irradiation mode (see Table 1).

The thermal neutron flux measurement was performed at 5 mm depth-increments from the surface of the water phantom up to a depth of 53 mm. At depths greater than 53 mm, measurements were done at 10 mm depth-increments. When the measured thermal neutron flux reached more than 10^8 n/cm^2/s, only 10-second measurements were enough to satisfy acceptable statistical accuracy, i.e. 0.5% standard deviation. However, at depths where the flux went below 10^8 n/cm^2/s measurement times were flexibly adjusted in order to achieve the same statistical accuracy.

Fig. 10 shows the measured thermal neutron flux distribution by the paired SOF detector and the gold wire method. Note that the neutron flux measured by the gold wire method were corrected in reference to the measured value by the SOF detector at 38 mm because the rector power was expected to fluctuate up to a maximum of 5% on different days of measurement. From Fig. 10, it is found that the measured value by SOF detector is in good agreement with the gold wire measurement. For the gold wire method, it will take a few days to measure the thermal neutron flux from 10^6 to 10^9; this is inclusive of the irradiation time, waiting time for decay and measurement time. In contrast, it took only 15 min to obtain almost same data using the SOF detector. Moreover, the linearity of the SOF detector was confirmed in the range of 10^6–5×10^9 n/cm^2/s using appropriate correction methods.

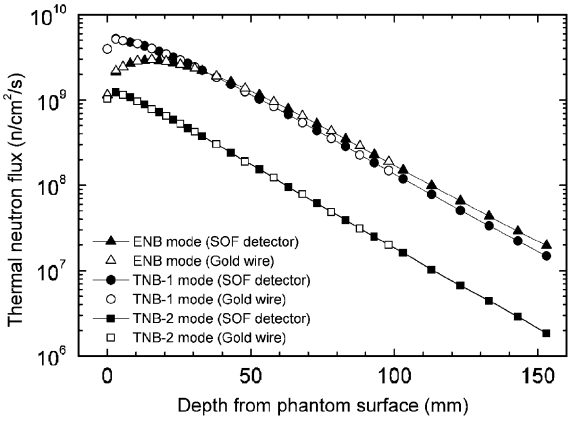

Fig. 10. The measured thermal neutron flux distribution by the paired SOF detector and the gold wire method. The values measured by the gold wire method were corrected in reference to the measured value by the SOF detector at 38 mm.

5. Conclusion

In order to upgrade the SOF detector system, we tried compensating for the gamma-ray and fast-neutron contribution by using a paired SOF detector, one with a neutron converter and the other without. The paired SOF was effective at low thermal neutron flux. Moreover, in order to correct for count-drop at high counting rate, the non-paralyzable system model was applied to the paired SOF detector. As a result, the dynamic range of linearity was confirmed in the order of magnitude of 10^4. For this system, a dynamic range of linearity up to an order of magnitude of 10^5 should be achievable. We confirmed that this upgraded SOF detector is useful for the evaluation of BNCT irradiation field.

Acknowledgement

This research is supported by a Grant-in-Aid for Young Scientists (A) (#16689022) by the Ministry of Education, Culture, Sports, Science and Technology.

Reference

[1] A.J. Peurrung, Nucl. Instr. and Meth. A 443 (2000) 400.

[2] C. Mori, A. Uritani, H. Miyahara, T. Iguchi, S. Shiroya, K. Kobayashi, E. Takada, R.F. Fleming, Y.K. Dewaraja, D. Stuenkel, G.F. Knoll, Nucl. Instr. and Meth. A 422 (1999) 129.
[3] M. Ishikawa, K. Ono, Y. Sakurai, H. Unesaki, A. Uritani, G. Bengua, T. Kobayashi, K. Tanaka, T. Kosako, Appl. Radiat. Isot. 61 (5) (2004) 775.
[4] K. Yamamoto, H. Kumada, T. Kishi, Y. Torii, Measurement of two-dimensional thermal neutron flux in a water phantom and evaluation of dose distribution characteristics, JAERI-Tech 2001–015 (2001) (in Japanese).